

Methanol synthesis from CO₂ via hydrogenation route: Thermodynamics and process development with techno-economic feasibility analysis

Suresh Kanuri*, Jha Deeptank Vinodkumar*, Santanu Prasad Datta**, Chanchal Chakraborty***, Sounak Roy***, Satyapaul Amarthaluri Singh*, and Srikanta Dinda*,†

*Department of Chemical Engineering, Birla Institute of Technology and Science (BITS) Pilani, Hyderabad Campus, Hyderabad, Telangana-500078, India

**Department of Mechanical Engineering, Birla Institute of Technology and Science (BITS) Pilani, Hyderabad Campus, Hyderabad, Telangana-500078, India

***Department of Chemistry, Birla Institute of Technology and Science (BITS) Pilani, Hyderabad Campus, Hyderabad, Telangana-500078, India

(Received 27 July 2022 • Revised 9 September 2022 • Accepted 25 September 2022)

Abstract—The present study investigated the thermodynamic and economic feasibility of methanol synthesis reactions from CO₂ and H₂. Three reactions, namely CO₂ hydrogenation to methanol, reverse-water-gas-shift (RWGS) and methanol decomposition reaction, were considered. The effect of temperature, pressure and H₂/CO₂ mole ratio on CO₂ conversion and methanol selectivity was examined explicitly. The simulation results were compared with experimental data. A conceptual process design for methanol synthesis from CO₂ was developed using an Aspen Plus process simulator. At 250 °C and 50 bar, the analysis shows about 73% CO₂ conversion and 99.7% CH₃OH selectivity for a recycling ratio of 0.9. A techno-economic feasibility study was performed to understand the influence of feed and product cost, recycling ratio and plant throughput, on plant profit margins. The study revealed that the proposed process might be economically viable if the H₂ price is lower than 1,500 \$/ton and/or with a methanol production capacity of more than 250 tons/day.

Keywords: CO₂ Hydrogenation, Methanol Synthesis, Aspen Simulation, Equilibrium Analysis, Economic Analysis

INTRODUCTION

An increasing trend in global warming, a declining trend of fossil fuel reserves and the need for an alternative to fossil fuels are the challenges of the twenty-first century. The CO₂ concentration in the atmosphere has increased to about 420 ppm from the pre-industrialization level of about 280 ppm [1,2]. In this context, the scientific community has concentrated on two key technologies, namely carbon capture and storage (CCS) and carbon capture and utilization (CCU) [3-5]. To reduce CO₂ concentration in the atmosphere, CCU technology has emerged as a more appealing alternative than CCS [6]. CO₂ hydrogenation pathways have become essential for producing useful chemicals, such as syngas, methane, methanol, ethanol, dimethyl ether and formic acid [7,8]. Methanol synthesis from CO₂ hydrogenation receives more emphasis due to environmental friendliness, lack of toxic emissions and other uses of methanol [9]. Methanol is used as a solvent and a raw material for the production of a wide range of chemicals, including formaldehyde, acetic acid, methyl methacrylate, dimethyl terephthalate, methylamines, dimethyl ether, and methyl-tert-butyl ether [10,11].

Synthesis of methanol from CO₂ hydrogenation using Cu, Ag, Au and Pd-based catalysts has been investigated by numerous scientists

[12-15]. Witoon et al. studied the CO₂ hydrogenation to methanol using Cu/ZnO catalyst at 180 °C and 20 bar pressure. The study revealed about 98% methanol selectivity for a CO₂ conversion of 5% [12]. The increase of oxygen vacancies in CeO₂ by Pd and Zn resulted 100% methanol selectivity and 7.7% CO₂ conversion at 220 °C and 30 bar [13]. Rui et al. investigated the CO₂ hydrogenation reaction over Au/In₂O₃ catalyst and achieved 100% methanol selectivity at 225 °C and 50 bar pressure; however, CO₂ conversion was limited to 1.3% [14]. In the majority of the experimental investigations on hydrogenation of CO₂ for methanol synthesis using different catalysts, the experiments were performed under pressures ranging between 1 bar to 150 bar [16]. Though, in most of the studies, the obtained selectivity of methanol was more than 98%, the CO₂ conversion was limited to below 10% only [17]. A thermodynamic analysis of any reactive system can anticipate the feasibility of maximum yield of desired products and also the optimum conditions required to obtain the desired yield. Hence, understanding the thermodynamic aspects of methanol synthesis reactions is essential for strategic development of a catalytic CO₂ hydrogenation process.

A few simulation studies have been performed to find optimum values of operating parameters for large-scale methanol productions [18-28]. Leonzio has simulated the influences of reaction pressure, temperature, feed (H₂/CO₂) molar ratio and recycle ratio on methanol synthesis rate [18]. The cost of methanol production from gasification of vacuum residue is about 14% lower compared to a steam

†To whom correspondence should be addressed.

E-mail: srikantadinda@gmail.com

Copyright by The Korean Institute of Chemical Engineers.

reforming route [21]. A response surface optimization method showed that the methanol production cost can be about 565 \$/ton if a reactor operates at 183 °C and 58 bar pressure [22]. Atsonios et al. studied the impact of H₂ cost on the economic viability of methanol production from CO₂ [23]. Bellotti et al. used ECoMP software to simulate the performance of a methanol plant of capacity 137 tons/day. The study revealed that the plant profitability was greatly influenced by the H₂ cost and methanol selling price [24]. Nyari et al. studied the energy and mass balance analysis of a methanol production plant of capacity 5,000 tons/day using an Aspen Plus software. The study concluded that the price of H₂ has a significant impact on the production cost of methanol [25]. Son et al. studied the heat transfer effect of a pilot-scale methanol synthesis reactor [26]. Jeong et al. proposed a methanol synthesis process by utilizing the exhaust CO₂ from an engine plant [28]. Rafati et al. performed a techno-economic analysis of a methanol synthesis process using an Aspen Plus software [29]. Gao et al. conducted the techno-economic analysis of methanol synthesis process using the by-product gases from steel industries. The six-tenth factor approach was used to estimate the costs of the major equipment [30]. In most of the investigations, it is reported that the prices of H₂ and the market value of methanol play a crucial role for a sustainable methanol plant. Converting CO₂ into methanol requires cost-effective production of H₂. H₂ can be synthesized via a variety of processes, including water electrolysis, steam methane reforming, coal gasification, and methane pyrolysis [31]. Noh et al. studied the production of CO₂-free H₂ from CH₄ by using a multistage bubble column reactor and molten alloy catalyst at around 980 °C [32]. Pirrone et al. reported the suitability of sun-driven water-splitting devices like photocatalytic, photoelectrochemical and photovoltaic-electrolyzer for H₂ production [33]. Brigljevic et al. investigated the efficacy of H₂ production from various organic hydrogen carriers like biphenyl/di-phenylmethane, 2-(N-Methylbenzyl)pyridine, N-phenylcarbazole, and the estimated price of H₂ production was in the order of 3,500 \$/ton [34].

In the present work, the thermodynamic feasibility of the CO₂ hydrogenation into methanol synthesis reaction is investigated, considering two more critical reactions, namely reverse-water-gas-shift (RWGS) and methanol decomposition reactions. The focus of the present work is the utilization of CO₂ for the production of methanol. The effects of various parameters, such as reactor temperature, pressure, and feed composition, on CO₂ conversion and methanol selectivity was examined explicitly. The simulated data are presented in bar charts to understand the optimum operating conditions for a particular value of CO₂ conversion and methanol selectivity. An Aspen Plus process simulator was used to develop a conceptual process design for methanol synthesis from CO₂. The formation of CO through the RWGS reaction and its avoidance is not exclusively reported in literature. In this manuscript, we studied the influence of water-gas-shift reaction to minimize toxic CO concentration in the effluent of a methanol plant. The simulation results were compared with the literature-reported experimental results. Further, the influence of recycle stream on maximization of methanol yields and minimization of CO formation was investigated considering an optimized flow diagram. Also, the impact of feed (CO₂ and H₂) and methanol (CH₃OH) cost, recycling ratio and plant capacity on

profit margins of a methanol plant was analyzed in detail.

METHODOLOGY

1. Equilibrium Studies Investigation

The Gibbs free energy minimization approach was adopted to define the equilibrium composition of a reaction system. The Gibbs free energy (G) of a system is minimum at equilibrium and its differential is equal to zero. The equilibrium reactor model (R_{Equil}) in the Aspen Plus simulator was used in the work. The Peng-Robinson equation of state (PENG-ROB EOS) model was considered to introduce non-ideal behavior in the Gibbs energy values [35]. To obtain a better understanding of the methanol synthesis *via* CO₂ hydrogenation route, the three reactions, namely methanol synthesis from CO₂ hydrogenation (Eq. (1)), RWGS (Eq. (2)) and CH₃OH decomposition (Eq. (3)) reactions, were considered in the entire analysis.



The following expressions are used to define CO₂ conversion (Eq. (4)), methanol selectivity (Eq. (5)), methanol yield (Eq. (6)), CO selectivity (Eq. (7)). The simulations were carried out under isothermal conditions. The results are shown in section 3 in terms of CO₂ conversion, CH₃OH yield and selectivity of both CH₃OH and CO for specific reaction conditions.

$$\text{Conversion of CO}_2 \text{ (\%)} = \left[1 - \frac{F_{\text{CO}_2, \text{out}}}{F_{\text{CO}_2, \text{in}}} \right] \times 100 \quad (4)$$

$$\text{Selectivity of CH}_3\text{OH (\%)} = \left[\frac{F_{\text{CH}_3\text{OH}, \text{out}}}{F_{\text{CH}_3\text{OH}, \text{out}} + F_{\text{CO}, \text{out}}} \right] \times 100 \quad (5)$$

$$\text{Yield of CH}_3\text{OH (\%)} = \left[\frac{F_{\text{CH}_3\text{OH}, \text{out}}}{F_{\text{CO}_2, \text{in}}} \right] \times 100 \quad (6)$$

$$\text{Selectivity of CO (\%)} = \left[\frac{F_{\text{CO}, \text{out}}}{F_{\text{CH}_3\text{OH}, \text{out}} + F_{\text{CO}, \text{out}}} \right] \times 100 \quad (7)$$

where $F_{i, \text{in}}$ and $F_{i, \text{out}}$ ($i = \text{CO}_2, \text{CO}, \text{CH}_3\text{OH}$) are the reactor inlet and outlet molar flowrates of species 'i', respectively.

2. CO₂ to CH₃OH Process Plant Development

A methanol synthesis process typically includes feed section, methanol reactor, product purification units. The CH₃OH synthesis and purification process flowsheet is proposed to maximize CO₂ conversion and CH₃OH selectivity and minimize CO levels. The Aspen Process Economic Analyzer (ASPEN PEA) and six-tenth factor method were used to estimate the capital investments of major units such as multi-stage compressor, CH₃OH reactor, heat exchanger, gas-liquid separator, distillation column, and WGSR.

RESULTS AND DISCUSSION

We performed a simulation study on methanol production from CO₂ and H₂. The study was performed for a wide range of temperature (50 °C to 450 °C), pressure (1 bar to 50 bar), H₂-to-CO₂ mole

ratio (3 to 15), recycling ratio (0.0 to 0.9), to examine the influence of major operating parameters on CO₂ conversion and methanol selectivity. The study also includes a process design of a methanol synthesis plant using an Aspen Plus process simulator and its techno-economic feasibility analysis. About 15% of the simulations were repeated to check the difference in CO₂ conversion and methanol selectivity. Between the repeated simulations, the observed deviation was less than 2%. The variation is mainly due to the truncated value of the physico-chemical property of the components or the property relationship used in the simulation. It was also found that for an identical operating condition (temperature, pressure, and H₂/CO₂ ratio), the Peng-Robinson equation of state and Soave-Redlich-Kwong equation of state showed nearly a similar value of CO₂ conversion and methanol selectivity with less than 2% deviation. In techno-economic analysis, the reported data are truncated up to decimal values in some cases. The calculated value of economic parameters, profit margin, payback period, etc., may vary within $\pm 3\%$ for second or third decimal truncated values.

1. Equilibrium Analysis

1-1. Effect of Temperature on Enthalpy, Entropy and Gibbs Free Energy Change

A shift in Gibbs free energy governs the spontaneity of a chemical reaction. Fig. 1(a)-(c) shows the effect of temperature on enthalpy (ΔH), entropy (ΔS) and Gibbs free energy (ΔG) change of the CO₂ hydrogenation, RWGS and CH₃OH decomposition reactions under 1 bar pressure. As observed in Fig. 1(a) and Fig. 1(b), the ΔH and ΔS values for CO₂ hydrogenation reaction are less than zero as the temperature increases from 25 °C to 450 °C. This signifies that the CO₂ hydrogenation to methanol is an exothermic reac-

tion. In contrast, the ΔH and ΔS values for both the RWGS and CH₃OH decomposition reactions are greater than zero for the studied temperature range. This implies that the RWGS and CH₃OH decomposition reactions are endothermic with increasing molecular disorder. As shown in Fig. 1(c), the ΔG for methanol synthesis reaction is greater than zero and increases with temperature, which means this reaction is favorable at low temperatures. The positive value of ΔG for the RWGS reaction and the decreasing trend with temperature implies that the reaction is favorable at high temperatures.

1-2. Influence of Temperature and Pressure on CO₂ Conversion and CH₃OH Selectivity

According to Le Chatelier's principle and thermodynamic analysis, high pressures and low temperatures are the favorable conditions for higher methanol selectivity (Eq. (1)). RWGS and methanol decomposition reactions are also limited under these conditions due to endothermicity. Hence, high pressures and low temperatures can be the optimum operating conditions to improve methanol selectivity and, at the same time, to reduce CO selectivity. The impact of temperature and pressure on CO₂ conversion, CH₃OH selectivity and CO selectivity was examined and the outcomes are shown in Fig. 2(a)-(c). The plots show that the equilibrium conversion of CO₂ is regulated by both temperature and pressure. With the increase of temperature, the methanol formation reaction becomes less favored, the RWGS and methanol decomposition reactions become more favored, resulting in U-shaped curves in the CO₂ conversion patterns. Increased pressure enhances CO₂ conversion in the low-temperature zone (e.g., 100 °C to 350 °C). However, for high temperatures (between 350 °C and 450 °C), the influence of pres-

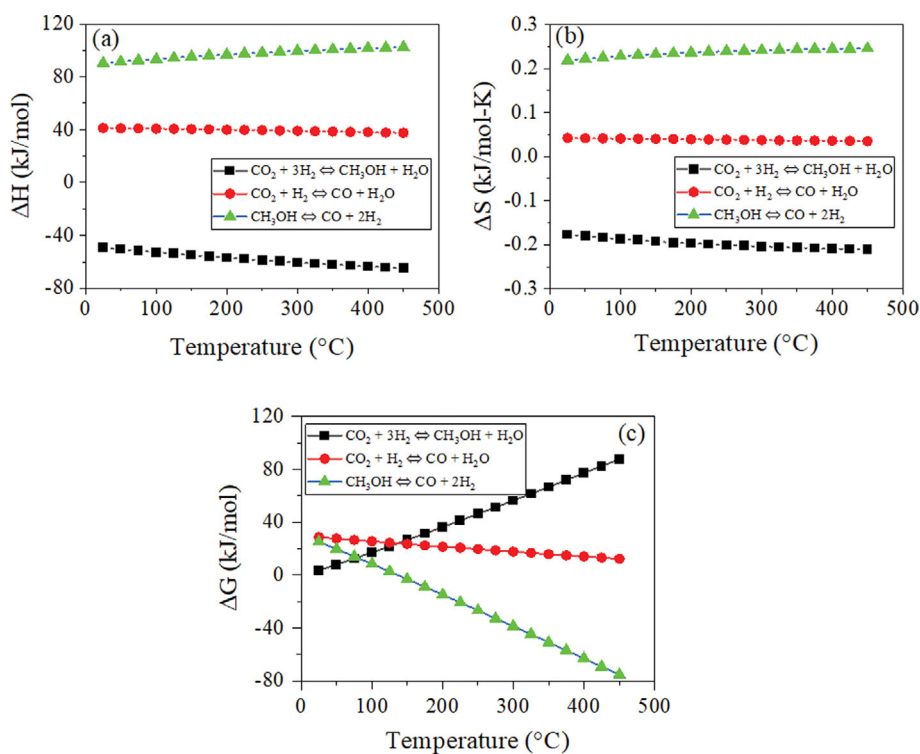


Fig. 1. Effect of temperature on (a) ΔH , (b) ΔS , (c) ΔG for CO₂ hydrogenation, RWGS and CH₃OH decomposition reactions under 1 bar pressure.

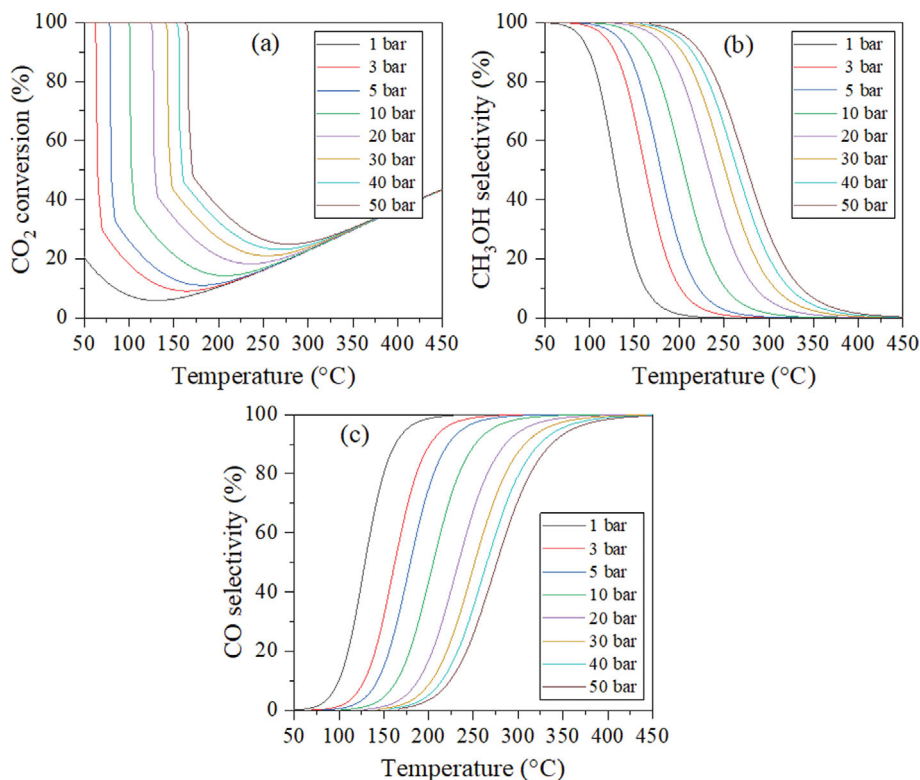


Fig. 2. Effect of pressure and temperature on (a) CO₂ conversion, (b) CH₃OH selectivity, (c) CO selectivity for H₂/CO₂ mole ratio of 3.

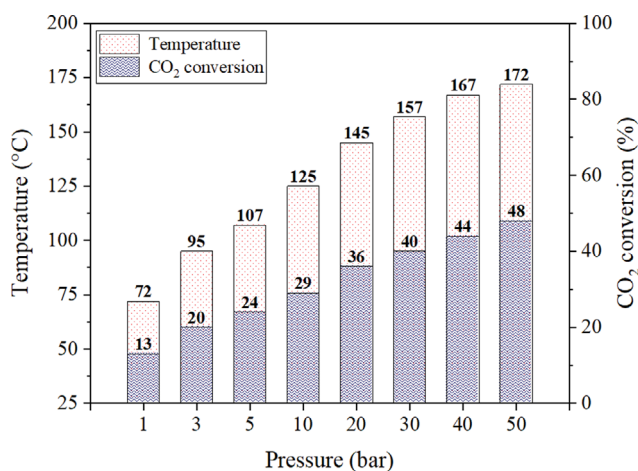


Fig. 3. Effect of pressure on CO₂ conversion and reactor temperature for 99% CH₃OH selectivity for H₂/CO₂ mole ratio of 3.

sure on CO₂ conversion is almost insignificant and the CO₂ conversion curves eventually converge at higher temperatures. Methanol selectivity is improved by increasing pressure, whereas the RWGS and methanol decomposition reactions are mostly unchanged. This illustrates that, as pressure increases, both the CH₃OH and CO selectivity curves shift to extremely high temperatures. A similar kind of phenomenon was also noted by Ahmad et al. [36] and Stangeland et al. [37] with Soave-Redlich-Kwong equation of state.

The effect of pressure on optimum value of operating temperature and CO₂ conversion to achieve 99% CH₃OH selectivity is presented in Fig. 3. As the pressure increased from 1 bar to 50 bar, the

CO₂ conversion increased from 13% to 48%. Hence, to obtain 99% methanol selectivity and 48% CO₂ conversion, the optimum value of reaction temperature and pressure is 172 °C and 50 bar, respectively, for the H₂/CO₂ mole ratio of 3.

1-3. Influence of Feed Gas Composition on CO₂ Conversion and CH₃OH Selectivity

To investigate the influence of feed composition on CO₂ conversion and CH₃OH selectivity, the H₂/CO₂ mole ratio was varied between 3 to 15 for a fixed value of reactor pressure at 50 bar. The simulation was performed for a temperature range between 150 °C to 400 °C and the results are shown in Fig. 4(a)-(c). The plots show that the increase of H₂ partial pressure promotes both the CO₂ conversion and CH₃OH selectivity. The methanol formation from CO₂ decreased as the temperature increased and, consequently, the consumption of CO₂ decreased. Hence, the increase in CO₂ conversion at higher temperatures (>280 °C) indicates that extra H₂ promotes the RWGS reaction. A significant change in CO₂ conversion was observed as the H₂/CO₂ mole ratio was increased from 3 to 9. Further increase of H₂/CO₂ ratio from 9 to 15, the improvement in CO₂ conversions slowly decreased.

Fig. 5 depicts the influence of feed gas composition on CO₂ conversion and optimum temperature to obtain 99% CH₃OH selectivity under 50 bar reactor pressure. The simulation shows that the CO₂ conversion improved from 48% to 83% when the H₂/CO₂ mole ratio increased from 3 to 15. About 83% CO₂ conversion and 99% methanol selectivity can be achievable at 186 °C under 50 bar pressure, and with an H₂/CO₂ mole ratio of 15. Though the boosting of H₂ partial pressure promotes the conversion of CO₂, it has a detrimental impact on process economics.

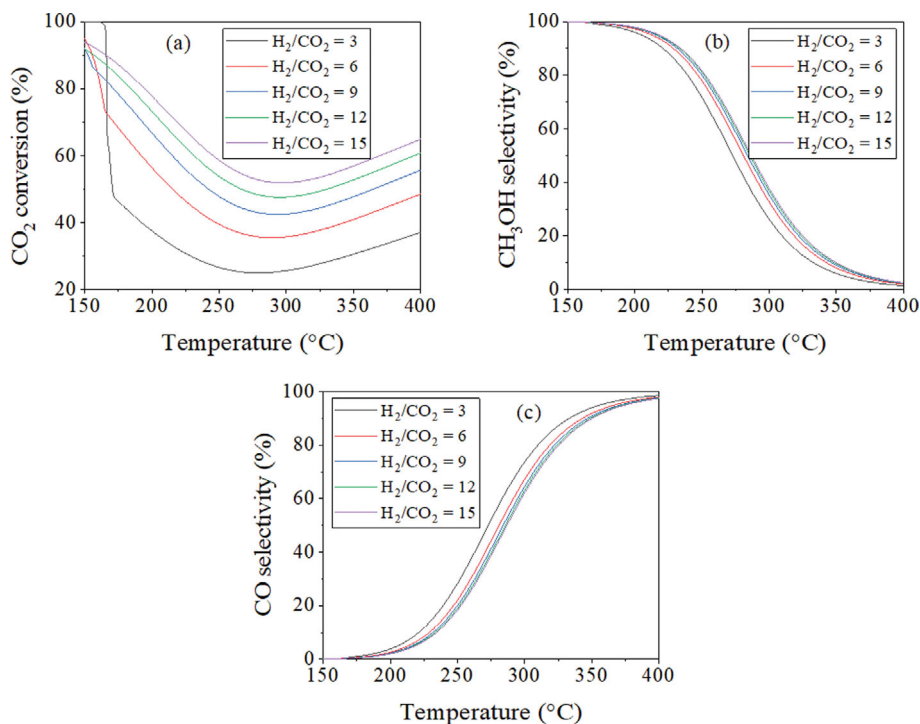


Fig. 4. Effect of H₂/CO₂ mole ratio on (a) CO₂ conversion, (b) CH₃OH selectivity, (c) CO selectivity at 50 bar pressure

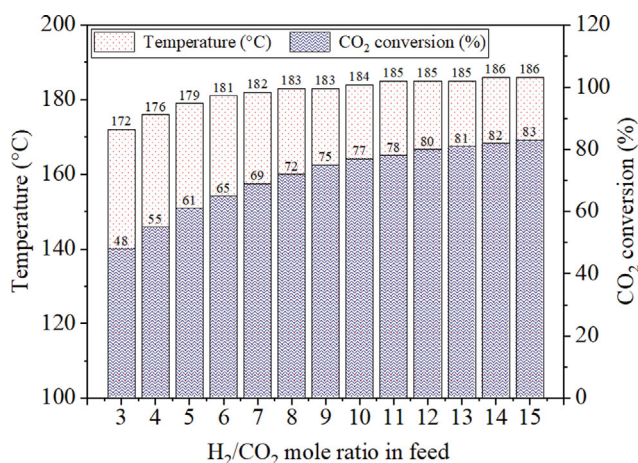


Fig. 5. Effect of H₂/CO₂ mole ratio on CO₂ conversion and desired temperature to achieve 99% CH₃OH selectivity under 50 bar pressure.

1-4. Comparison of CO₂ Conversion and CH₃OH Selectivity

For a similar range of reactor temperature, pressure and feed gas composition, the simulation predicted CO₂ conversion was compared with the experimental results, as shown in Fig. 6(a). The experimentally obtained conversion and selectivity are reported for Au/In₂O₃ [14] and Cu/ZnO/Al₂O₃ [16] catalysts. The figure shows that the simulation results obtained from the present investigation are comparable with the data reported by Stangeland et al. [37]. However, a substantial difference between the theoretical and experimental values of CO₂ conversion is noted. The difference is greater at low temperatures and it reduces gradually with the increase of

reactor temperature. The lower value of CO₂ conversion in the presence of catalysts can be related to the weak activity of the catalysts. Fig. 6(b) shows a comparison between the equilibrium and experimental selectivity of CH₃OH. Though the Cu/ZnO/Al₂O₃ catalyst shows a significant deviation in CH₃OH selectivity, the difference is relatively less for the Au/In₂O₃ catalyst. Also, the methanol selectivity over Au/In₂O₃ catalyst is more than the equilibrium selectivity of CH₃OH, which may be due to the presence of Au^{δ+}-In₂O_{3-x} interfacial sites in the Au/In₂O₃ catalyst. Therefore, to enhance the CO₂ conversion and CH₃OH selectivity, it is essential to develop an efficient, highly-stable and low-cost catalyst.

A summary on CO₂ conversion and CH₃OH selectivity is shown in Table 1. At higher temperatures (>230 °C), though the conversion of CO₂ is relatively greater, the selectivity of methanol is less than 90% in most cases. It indicates that a significant amount of CO₂ was converted into undesired products like CO and CH₄. However, due to the chemically inert state of CO₂, experimental investigation often requires a temperature greater than 220 °C to promote CO₂ activation [38,39].

2. Development of Process Flowsheet for CO₂ to CH₃OH Synthesis Process

In this work, a process flowsheet on CH₃OH synthesis is proposed to maximize CO₂ conversion and CH₃OH selectivity. Aspen Plus simulator was used to develop the process flowsheet for the CO₂ hydrogenation reaction, as shown in Fig. 7. The feed gas and recycle gas streams are mixed in the mixer and then compressed by a multi-stage compressor with intermediate cooling to achieve the operating condition (250 °C and 50 bar) of the methanol reactor. The outflow stream from the reactor is passed through a shell and tube-type heat exchanger to reduce the temperature of the

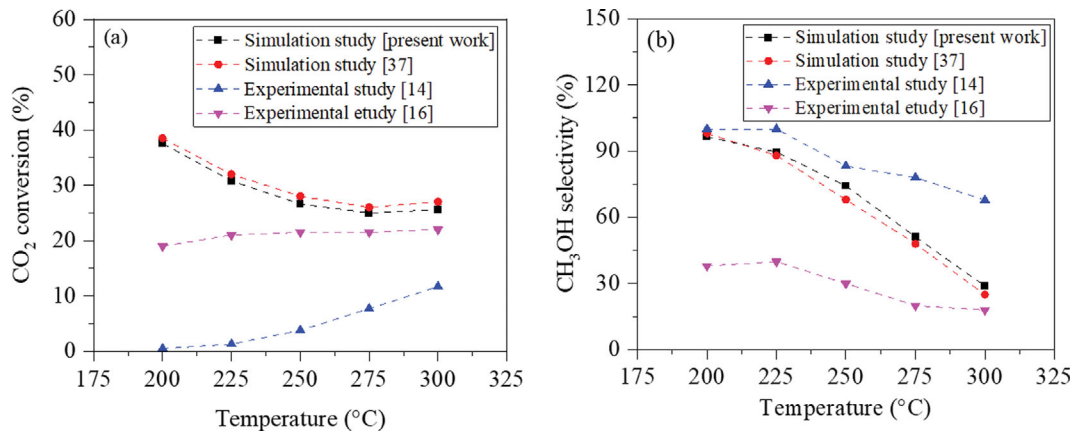


Fig. 6. Simulation and experimental results of (a) CO₂ conversion, (b) CH₃OH selectivity.

Table 1. A comparison between simulation and experimental findings on CO₂ conversion and CH₃OH selectivity for methanol synthesis via CO₂ hydrogenation

Catalyst	H ₂ : CO ₂ mole ratio	T _R (°C)	P _R (bar)	X _{CO₂} (%)	S _{MeOH} (%)	Reference
Cu/ZnO	3	180	20	5	98	[12]
PdZn/CeO ₂	3	220	30	7.7	100	[13]
Au/In ₂ O ₃	3	225	50	1.3	100	[14]
Cu/ZnO/Al ₂ O ₃	3	240	46	20	40	[16]
Pd-Zn/CNTs	3	250	30	6.3	99	[40]
Cu/ZnO/Al ₂ O ₃	3	170	50	25	73	[41]
Cu-ZrO ₂	3	250	30	12	40	[42]
Cu-ZnO- ZrO ₂	3	250	40	17	30	[43]
Au/In ₂ O ₃ -ZrO ₂	3	250	50	6.1	90	[44]
-	3	200	50	39	98	[37]
-	3	250	50	28	68	[37]
-	3	172	50	48	99	[present work]
-	3	250	50	28	72	[present work]
-	10	184	50	77	99	[present work]
-	10	250	50	51	80	[present work]

where, T_R=reaction temperature; P_R=reaction pressure; X_{CO₂}=CO₂ conversion, S_{MeOH}=methanol selectivity.

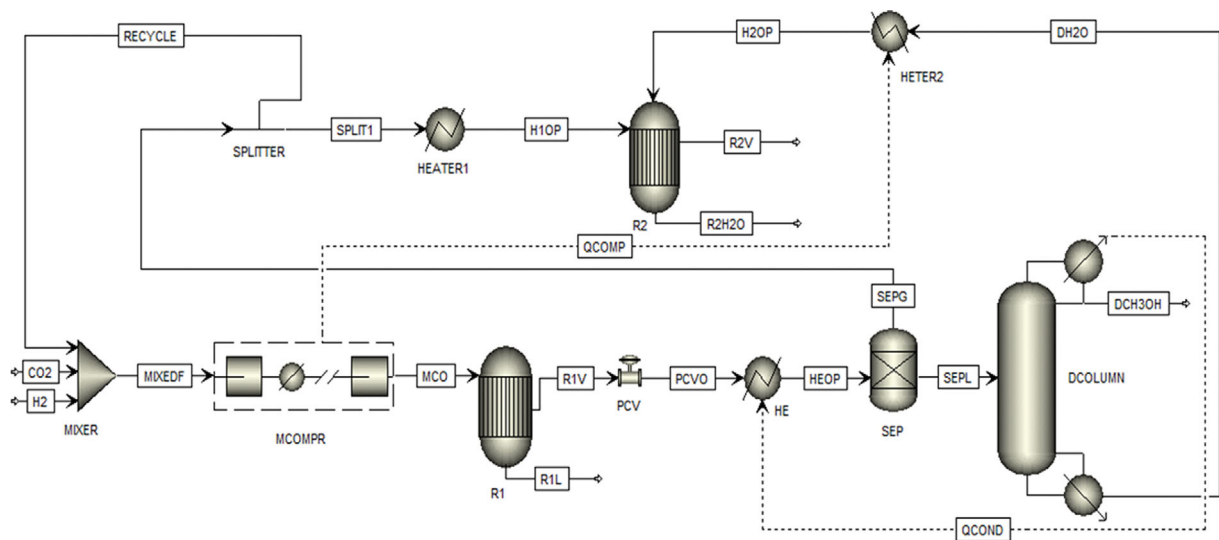


Fig. 7. A process flowsheet of methanol synthesis via CO₂ hydrogenation route.

stream to about 50 °C before sending it into the separator. The crude methanol (mixture of CH₃OH and H₂O) is separated in the separator and fed to the distillation unit to enhance the methanol purity. Part of the unreacted CO₂, H₂ and *in-situ* formed CO gas mixture obtained from the separator is recycled into the mixing unit

to improve the CO₂ conversion and methanol yield. To minimize the accumulation of undesired products in the reaction loop, the leftover fraction of gases (CO₂, H₂, and CO) are purged and sent to the water-gas-shift-reactor (WGSR), where the CO reacts with water to produce CO₂ and H₂. The distillation column was designed to

Table 2. Various parameters and their ranges used for Aspen simulation

Process	Flowsheet code	Operating conditions
Mixer	MIXER	- T=25 °C, P=1 bar
Compressor	MCOMPR	- Outflow conditions: - T=250 °C, P=50 bar, - Number of stages=2
Reactor (Methanol)	R ₁ (REquil)	- T=250 °C, P=50 bar, - Recycle ratio range: 0.0-0.9, - Reactions: CO ₂ +3H ₂ ⇌CH ₃ OH+H ₂ O CO ₂ +H ₂ ⇌CO+H ₂ O CH ₃ OH⇌CO+2H ₂ - Base method: PENG-ROB EOS.
Pressure changer	PCV	- Inflow: T=250 °C, P=50 bar, - Outflow: T=247 °C, P=1 bar,
Heat exchanger	HE	- Inflow: T=247 °C, P=1 bar, - Outflow: T=50 °C, P=1 bar.
Separator	SEP	- T=50 °C, P=1 bar.
Distillation column	DCOLUMN (RadFrac)	- No. of stages: 45, - Condenser type: total condenser, - Reboiler type: kettle, - Feed tray: 36 th , - Reflux ratio (R): 2.75, - Bottoms to feed ratio (B/F): 0.6.
Splitter	SPLITTER	- Recycle stream split fraction range: 0.0-0.9.
Heater-1	HEATER	- Inflow: T=50 °C, P=1 bar, - Outflow: T=230 °C, P=1 bar
Heater-2	HEATER	- Outflow: T=230 °C, P=1 bar.
Reactor (WGSR)	R ₂ (REquil)	- T=230 °C, P=1 bar - Reaction: CO+H ₂ O⇌CO ₂ +H ₂ - Base method: PENG-ROB EOS.

Table 3. Effect of recycle on the performance of the proposed methanol synthesis plant

Recycle ratio	Feed rate (tons/day)	H ₂ /CO ₂ mole ratio at mixer exit	X _{CO₂} (%)	CH ₃ OH yield (tons/day)	CO concentration (ppm)
0.0	820	3.00	25.2	100	18,231
0.1	820	3.02	26.6	110	16,760
0.2	820	3.03	28.2	122	15,154
0.3	820	3.05	30.3	136	13,411
0.4	820	3.07	32.9	154	11,535
0.5	820	3.08	36.4	176	9,541
0.6	820	3.10	41.2	205	7,456
0.7	820	3.12	47.9	244	5,325
0.8	820	3.14	57.8	299	3,215
0.9	820	3.16	73.2	383	1,253

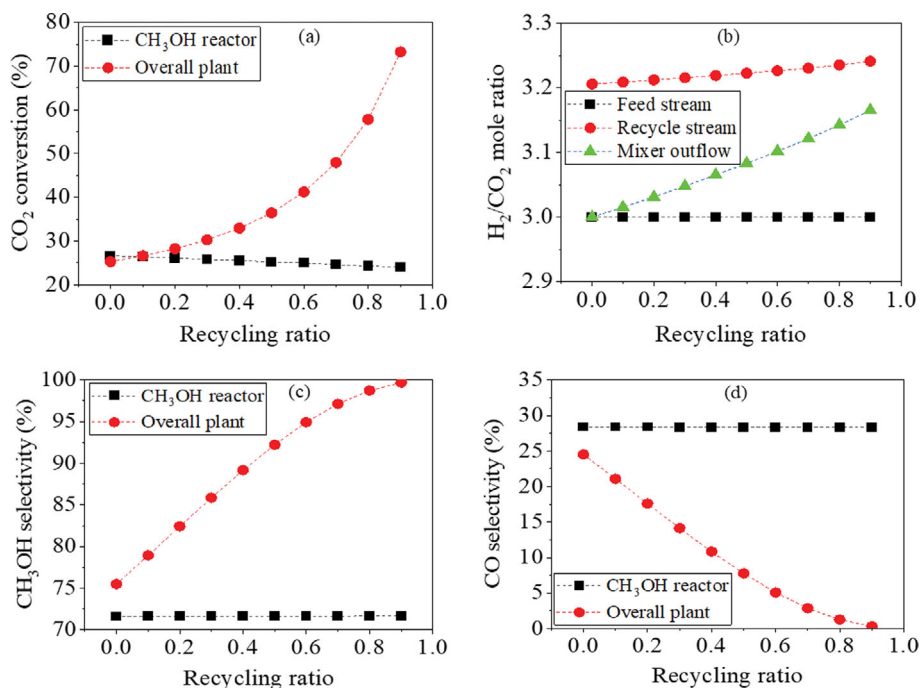


Fig. 8. Effect of recycling ratio on (a) CO₂ conversion, (b) H₂/CO₂ mole ratio, (c) CH₃OH selectivity, (d) CO selectivity at 250 °C and 50 bar pressure.

obtain more than 99.9% methanol purity for any value of gas recycle ratio. The details of the operating parameters and their ranges used in the present simulation are given in Table 2.

2-1. Effect of Recycle Ratio on CO₂ Conversion, CH₃OH, and CO Outflow Concentration

To study the influence of recycling ratio on CO₂ conversion and CH₃OH yield from the proposed methanol synthesis plant, simulations were performed for different values of recycle ratio for a capacity of 100 tons/day of methanol production. The estimated value of feed gas requirement for the 100 tons/day methanol production process is 820 tons/day (CO₂ is 721 tons/day and H₂ is 99 tons/day). The simulation results (Table 3) show that the methanol production rate improved from 100 to 383 tons/day when the recycle ratio varied from 0.0 to 0.9 for a constant value of feed flow rate.

Fig. 8(a)-(d) shows the impact of gas recycling ratio on CO₂ conversion, methanol selectivity, CO selectivity and H₂/CO₂ mole ratio at 250 °C and 50 bar pressure. Fig. 8(a) shows that the conversion of CO₂ from the overall plant increased gradually with recycling ratio. For a recycle ratio of greater than 0.1, the overall conversion of CO₂ is greater than the conversion obtained from the CH₃OH reactor. Due to the higher (>3) value of H₂/CO₂ mole ratio of the recycle stream, the CO₂ hydrogenation reaction in the CH₃OH reactor continues to improve with the increase of recycle ratio, which is ascertained from Fig. 8(b). As a result, the plant CO₂ conversion improved from 25% to 73%, while the recycle ratio increased from 0.0 to 0.9. Because of the water-gas-shift reactor (where CO reacts with H₂O to form CO₂ and H₂), the overall plant selectivity of methanol improved from 75% to 99.7% (Fig. 8(c)) and the CO selectivity decreased from 24.3% to 0.3% (Fig. 8(d)). At 90% recycling ratio, the analysis shows about 73% CO₂ conversion, 99.7%

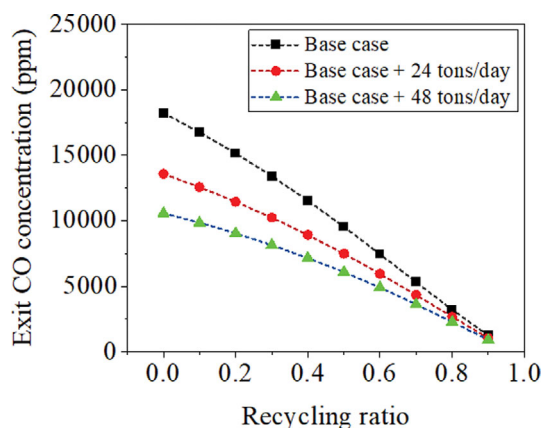


Fig. 9. Influence of water injection to WGSR on CO concentration.

CH₃OH selectivity and 0.3% CO selectivity.

The above base case simulation shows that the exit concentration of CO (ref. Table 3) from the overall plant is significantly high (>18,200 ppm without recycle). To reduce the concentration of CO below 1,000 ppm, simulations were performed with different amounts of water injection for the WGSR, and the results are shown in Fig. 9. For the base case, the internal water (water formed in methanol reactor and separated from the distillation column bottom) injection to the WGSR is about 56 tons/day. The analysis shows a decreasing trend in the CO concentration with the increase of external water injection. The reduction percentage is relatively low for the higher values of recycling ratio. At 0.9 recycling ratio, the CO concentration reduced to 918 ppm with the external water flow rate of 48 tons/day. From the analysis, it can be inferred that the increase of water injection to the WGSR alone cannot decrease the CO level

Table 4. Estimated costs of major equipment for the proposed CH₃OH synthesis plant for different values of recycle ratio

Equipment name	Equipment cost (M\$)									
	R=0.0	R=0.1	R=0.2	R=0.3	R=0.4	R=0.5	R=0.6	R=0.7	R=0.8	R=0.9
MCOMPR	2.17	2.28	2.40	2.54	2.71	2.92	3.16	3.48	3.89	4.47
R1 (CH ₃ OH Reactor)	1.98	2.08	2.20	2.33	2.48	2.67	2.90	3.18	3.56	4.09
HE	0.62	0.65	0.68	0.72	0.77	0.83	0.90	0.99	1.11	1.27
SEP	0.05	0.05	0.06	0.06	0.06	0.07	0.07	0.08	0.09	0.10
DCOLUMN	0.57	0.59	0.63	0.66	0.71	0.76	0.83	0.91	1.02	1.18
HEATER-1	0.17	0.17	0.17	0.16	0.16	0.15	0.14	0.14	0.12	0.09
HEATER-2	0.05	0.05	0.05	0.05	0.05	0.06	0.06	0.07	0.08	0.09
R2 (WGSR)	1.82	1.80	1.79	1.77	1.72	1.70	1.56	1.60	1.50	1.36
Total equipment cost	7.42	7.67	7.97	8.31	8.67	9.16	9.62	10.45	11.37	12.65
Total equipment delivered cost	8.16	8.44	8.77	9.14	9.54	10.08	10.59	11.50	12.51	13.91

M\$=Million USD; R=recycle ratio

Table 5. Estimated values of total capital investment cost

Category	Ratio factor	Cost (M\$)									
		R=0.0	R=0.1	R=0.2	R=0.3	R=0.4	R=0.5	R=0.6	R=0.7	R=0.8	R=0.9
Total equipment delivered	1.00	8.16	8.44	8.77	9.14	9.54	10.08	10.59	11.50	12.51	13.91
Equipment installation	0.47	3.84	3.97	4.12	4.29	4.48	4.74	4.98	5.40	5.88	6.54
Instrumentation	0.36	2.94	3.04	3.16	3.29	3.43	3.63	3.81	4.14	4.50	5.01
Piping	0.40	3.27	3.38	3.51	3.66	3.82	4.03	4.23	4.60	5.00	5.56
Electrical systems	0.11	0.90	0.93	0.96	1.01	1.05	1.11	1.16	1.26	1.38	1.53
Buildings	0.18	1.47	1.52	1.58	1.64	1.72	1.81	1.91	2.07	2.25	2.50
Yard improvements	0.10	0.82	0.84	0.88	0.91	0.95	1.01	1.06	1.15	1.25	1.39
Service facilities	0.50	4.08	4.22	4.38	4.57	4.77	5.04	5.29	5.75	6.26	6.95
Total direct cost (DC)		25.47	26.33	27.35	28.51	29.77	31.44	33.03	35.88	39.03	43.40
Engineering and supervision	0.33	2.69	2.78	2.89	3.02	3.15	3.33	3.49	3.79	4.13	4.59
Construction and expenses	0.41	3.35	3.46	3.59	3.75	3.91	4.13	4.34	4.71	5.13	5.70
Legal expenses	0.04	0.33	0.34	0.35	0.37	0.38	0.40	0.42	0.46	0.50	0.56
Contractors fee	0.22	1.80	1.86	1.93	2.01	2.10	2.22	2.33	2.53	2.75	3.06
Contingency	0.40	3.27	3.38	3.51	3.66	3.82	4.03	4.23	4.60	5.00	5.56
Total indirect cost (IC)		11.43	11.81	12.27	12.79	13.36	14.11	14.82	16.10	17.51	19.47
FCI		36.90	38.14	39.62	41.30	43.13	45.55	47.85	51.98	56.55	62.87
WCI	0.89	7.27	7.51	7.80	8.13	8.49	8.97	9.42	10.23	11.13	12.38
TCI		44.17	45.65	47.43	49.44	51.62	54.51	57.28	62.21	67.68	75.25

to below 100 ppm. An effective catalyst system is needed to reduce the CO concentration to an acceptable limit.

2-2. Techno-economic Analysis of the CO₂ to CH₃OH Process

To analyze the techno-economic feasibility of the methanol synthesis process, the Aspen Process Economic Analyzer (ASPEN PEA) and six-tenth factor (Eq. (8)) method [30,45] were used in the simulation. To calculate the cost of new equipment using six-tenth factor rule, the initial value of the equipment cost was taken from reported literature [25,30]. The cost of new equipment was recalculated using the chemical engineering plant cost index (CEPCI), as described in Eq. (8), to incorporate the capacity and price enhancement factors. The estimated value of capital investment cost of the major units, such as multi-stage compressor, methanol reactor, heat exchanger, gas-liquid separator, distillation column and WGSR

involved in the process flowsheet (Fig. 7) is presented in Table 4.

$$\left(\frac{P_{new}}{P_{ref}}\right) = \left(\frac{C_{new}}{C_{ref}}\right)^{(0.6)} \times \left(\frac{CEPCI_{new}}{CEPCI_{ref}}\right) \quad (8)$$

where P_{new} =purchased cost of new equipment, P_{ref} =purchased cost of reference equipment, C_{new} =capacity of new equipment, C_{ref} =capacity of reference equipment, $CEPCI_{new}$ =chemical engineering plant cost index (CEPCI) of new equipment in procurement year, $CEPCI_{ref}$ =CEPCI of reference equipment in the year of procurement.

The equipment delivered cost is considered as 10% of the equipment cost. The total capital investment (TCI) cost of the proposed plant is the sum of the fixed capital investment (FCI) and working capital investment (WCI) costs. The FCI of the plant is esti-

Table 6. Summary of economic assumptions considered in estimating TPC [30]

	Category	Economic assumption
C ₁	Raw materials	H ₂ =2,000 \$/ton, CO ₂ =10 \$/ton
C ₂	Utilities	Cooling water=0.0148 \$/ton, Electricity=0.06 \$/kWh
C ₃	Operation and maintenance	C _{3,1} +C _{3,2} +C _{3,3} +C _{3,4} +C _{3,5}
C _{3,1}	Operating labour	30 labour/shift, 3 shift/day, 8,000 \$/labour/year
C _{3,2}	Supervisory labour	20% of C _{3,1}
C _{3,3}	Maintenance and repairs	6% of FCI
C _{3,4}	Operating supplies	15% of C _{3,3}
C _{3,5}	laboratory charges	15% of C _{3,1}
C ₄	Patent and royalty	1% of TPC
C ₅	Depreciation	Recovery period 20 years, Salvage value 5%, Linear
C ₆	Tax and insurance	2% of FCI
C ₇	Plant overhead	60% of (C _{3,1} +C _{3,2} +C _{3,3})
C ₈	General expenses	C _{8,1} +C _{8,2} +C _{8,3}
C _{8,1}	Administration	20% of (C _{3,1} +C _{3,2} +C _{3,3})
C _{8,2}	Distribution and selling	5% of TPC
C _{8,3}	Research & development	4% TPC

Table 7. Economic analysis of proposed methanol plant

Recycle ratio	TCI (M\$)	Methanol sales (M\$/yr)	By-products sales (M\$/yr)	Total sales (M\$/yr)	TPC (M\$/yr)	TPP (M\$/yr)
0.0	44.2	18.3	59.0	77.3	90.5	-13.3
0.1	45.7	20.1	57.9	78.0	90.8	-12.7
0.2	47.4	22.3	56.6	78.9	91.0	-12.1
0.3	49.4	24.9	55.0	79.9	91.3	-11.4
0.4	51.6	28.1	53.0	81.2	91.7	-10.5
0.5	54.5	32.2	50.5	82.7	92.1	-9.4
0.6	57.3	37.5	47.1	84.6	92.6	-8.0
0.7	62.2	44.6	42.5	87.1	93.3	-6.2
0.8	67.7	54.7	35.9	90.6	94.2	-3.6
0.9	75.3	70.0	25.8	95.8	95.4	0.4

mated by adding the direct cost (DC) and indirect cost (IC). In the study, the DC, IC and WCI are determined by using the Peter and Timmerhaus suggested ratio factors (RF) [46]. The following expressions (Eq. (9)-(11)) are used to estimate the TCI and the outcomes are listed in Table 5.

$$TCI=FCI+WCI=(DC+IC)+WCI \quad (9)$$

$$DC \text{ and } IC=\Sigma(RF \times \text{per functional cost under each category}) \quad (10)$$

$$WCI=RF \times \text{Total equipment delivered cost} \quad (11)$$

Eq. (12) is used to compute the total product cost (TPC) based on the economic assumptions mentioned in Table 6. The depreciation cost is evaluated considering a linear depreciation approach for a 20-year recovery period and a salvage value of 5%.

$$TPC=C_1+C_2+C_3+C_4+C_5+C_6+C_7+C_8 \quad (12)$$

where C₁, C₂, C₃, C₄, C₅, C₆, C₇ and C₈ are the cost of raw materials, utility, operating and maintenance, patent and royalty, depreciation, tax and insurance, plant overhead and general expenses, re-

spectively.

The influence of raw materials (CO₂ and H₂) and product (CH₃OH) prices on total plant profit (TPP) and 'payback period (PPB)' of the proposed plant was analyzed. TPP is computed by subtracting the total product cost (TPC) from total product sales according to Eq. (13). The estimated values of TPC and TPP are summarized in Table 7. The ratio of the TCI to TPP is used to calculate the payback period of the project.

$$TPP=[(\text{methanol sales})+(\text{byproduct sales})-(\text{TPC})] \quad (13)$$

The estimated value of total capital investment (TCI) of the methanol plant is about 75.3 M\$ with a recycling ratio of 0.9, which is about 70% higher in comparison to the without recycling case. The analysis (Table 7) shows that the proposed plant will not give any profit margin up to the recycling ratio of 0.8 for the 100 tons/day methanol production capacity. However, for 0.9 recycling ratio, the plant shows about 0.4 M\$ of annual profit and the estimated payback period is remarkably high (around 200 years), which is not acceptable in reality. Hence, to enhance the profit margin and reduce

the payback period below ten years, it is necessary to explore various alternative sources of H₂ production at a lower price.

In the above analysis, the TPP and the payback period was estimated without considering any discount rate. Discount rate depends on several factors, such as geographical location, distance between the source and supply of feed and product, purity of feed and product, supplier and buyer status (government vs. private sector), duration of contract (shorter vs. longer duration) between the buyer and supplier, quantity of material (small quantity vs. large quantity). Typically, a discount rate may vary between 3% to 15%. A standard discounted cash flow analysis (DCFCA) has been performed to estimate the net present value (NPV) and discounted payback period (DPBP) of the proposed plant. Eq. (14) and Eq. (15) were used to estimate the net present value (NPV) and discounted payback period (DPBP), respectively.

$$NPV(t, n) = \sum_{t=0}^n \frac{CF_t}{(1+d)^t} \quad (14)$$

where, NPV=net present value, t=year of the cash flow, n=total number of years, CF=cash flow, and d=discount rate in percentage.

$$DPBP = N_y + \frac{|CF_n|}{CF_p} \quad (15)$$

where, N_y=number of years when last negative value of cumulative discounted cash flow takes place after initial investment, CF_n=last negative cumulative discounted cash flow, CF_p=discounted cash flow when first positive value of cumulative discounted cash flow.

The estimated values of NPV and DPBP for three different (100, 250 and 500 tons/day) capacity of methanol plant are presented in Table 8, along with other relevant details. Two representative values of discount rate (5% and 10%) and for a 20 year plant life are considered in the calculation. The internal rate of return (IRR) was determined by setting NPV=0 in Eq. (14). The negative value of NPV signifies that the plant operation is not economically viable for the said duration with specified throughput. The IRR value indicates the maximum percentage of discount rate permissible and at the end of 20 years the net present value will be zero with that discount rate.

2-3. Influence of Feed Cost, Products Cost and Plant Throughput Capacity on Plant Profit

The prices of raw materials and products have a significant impact on plant economics and profit margins. To find the sensitivity of the feed and product costs on plant profit, an economic analysis was performed for different values of feed (CO₂ and H₂) and product (CH₃OH) prices. Fig. 10(a) shows the impact of CO₂ pricing on the plant profits for a fixed value of H₂ (2,000 \$/ton) and methanol (500 \$/ton) prices. The figure shows that the plant profit increased with the increase of CO₂ price for a recycling ratio greater than 0.5. The analysis also indicates that the proposed plant would be economically viable with a CO₂ price of 30 \$/ton when the recycling ratio is greater than 0.8. Fig. 10(b) shows the influence of H₂ cost on plant profit for a fixed value of CO₂ (10 \$/ton) and methanol (500 \$/ton) prices. For all the recycle ratios, the plant profit increased with the decrease of H₂ cost. The analysis shows that the overall process becomes unprofitable if the H₂ price exceeds 1,500 \$/ton for the above-mentioned price of CO₂ and methanol. However, the proposed plant would be economically viable if the cost of H₂ is less than 1,000 \$/ton for the methanol throughput capacity of 100 tons/day.

Fig. 10(c) shows the influence of methanol cost on the plant profit for the fixed price of CO₂ (10 \$/ton) and H₂ (2,000 \$/ton). The result shows that the proposed plant is economically viable if the methanol price is more than 500 \$/ton for certain values of recycle ratio. The data shows that when the methanol price is 600 \$/ton, the plant is financially sustainable above recycling ratio of 0.6. The analysis also indicates that the breakeven point (no loss and no profit point) shifted towards the lower value of recycling ratio with the increase of methanol price.

Plant capacity/throughput is another influencing parameter on plant economics. Fig. 10(d) shows the impact of plant capacity on the plant profit for a fixed value of feed and product costs. The plots show that with the increase of methanol production capacity from 100 tons/day to 250 tons/day, the plant became economically viable above a recycling value of 0.8. The plot also shows that the profit margin increases with increasing throughputs and the breakeven point shifted towards lower recycling ratio. The estimated values of

Table 8. Estimated values of DPBP and IRR for 5% and 10% discount rates

Description	Case 1	Case 2	Case 3	Case 4	Case 5	Case 6
Plant capacity, TPD	100	250	500	100	250	500
Recycling ratio	0.9	0.9	0.9	0.9	0.9	0.9
TCI, M\$	75.3	130.5	197.6	75.3	130.5	197.6
Total sales, M\$/yr	95.8	239.8	478.7	95.8	239.8	478.7
TPC, M\$/yr	95.4	227.7	446.1	95.4	227.7	446.1
Net profit, M\$/yr	0.4	12.1	32.6	0.4	12.1	32.6
Depreciation, M\$/yr	0.6	1.1	1.7	0.6	1.1	1.7
Net cash flow, M\$/yr	1.0	13.3	34.3	1.0	13.3	34.3
PBP without discount, yr	75.3	9.8	5.8	75.3	9.8	5.8
Discount rate, %	5	5	5	10	10	10
NPV after 20 years, M\$	-62.8	34.6	230.1	-66.7	-17.7	94.6
DPBP, yr	-	13.9	7.0	-	-	9.0
IRR, %	-	8.0	16.6	-	-	16.6

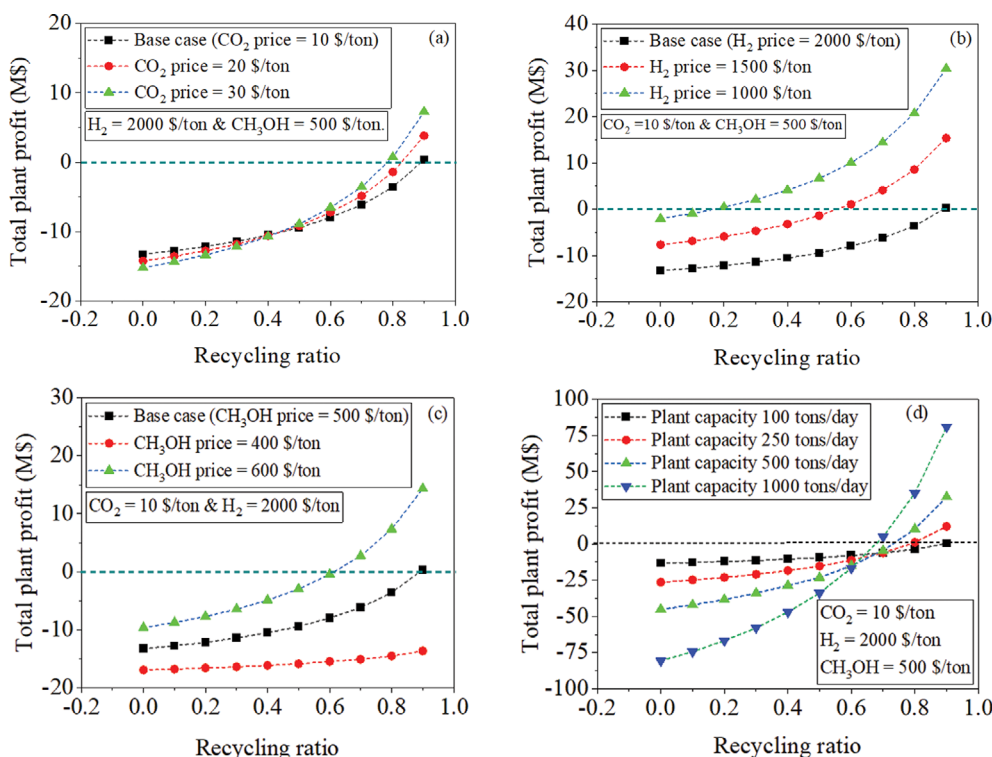


Fig. 10. Influence of (a) CO₂ cost, (b) H₂ cost, (c) methanol cost, (d) plant throughput capacity on plant profit.

Table 9. Values of profit margins and payback period for some selected conditions

	R=0.9	R=0.9	R=0.9	R=0.9	R=0.9	R=0.8	R=0.8
H ₂ price, \$/ton	2,000	1,000	1,000	2,000	1,500	1,500	1,500
CO ₂ price, \$/ton	10	10	10	10	10	10	10
Methanol price, \$/ton	500	500	400	500	400	400	500
Plant capacity, tons/day	100	100	100	500	500	500	100
Profit margin M\$/yr	0.4	30.4	16.4	32.6	37.8	16.5	8.6
Payback period without discount, yr	203	2.5	4.6	6.1	5.2	10.8	7.9
Payback period with 5% discount rate, yr	-	3.4	5.1	7.0	5.9	13.9	9.5

profit margin and payback period of the proposed plant for different combinations of feed and product price and plant capacity are shown in Table 9. In the estimation of discounted payback period, 5% discount rate was considered.

Therefore, from the aforementioned analysis, the cost of raw materials and products, plant capacity and recycling of unreacted feed play a vital role in enhancing the plant profit margins and economic sustainability. The techno-economic feasibility analysis revealed that the proposed plant would not be economically viable if the cost of CO₂ and H₂ is more than 10 \$/ton and 1,500 \$/ton, respectively, and methanol price is lower than 500 \$/ton for a 100 tons/day plant capacity. However, the proposed process might be profitable if the plant capacity increased even for the same feed and product costs. Gao et al. [30] and Zhang et al. [19] also reported a similar observation. If the cost of H₂ is reduced due to its easy availability and technology-enabled resources like methane steam reforming and electrolysis of water [47,48], the plant may be economically viable even for a 100 tons/day capacity.

CONCLUSIONS

A comprehensive study on thermodynamic aspects of CO₂ to methanol conversion, development of process flowsheet and techno-economic analysis is presented in this work. Based on the thermodynamic feasibility analysis, the methanol decomposition reaction showed a higher endothermicity than the RWGS reaction, while methanol formation from CO₂ is an exothermic reaction. The effects of critical parameters, such as pressure, temperature, feed gas composition on CO₂ conversion and methanol selectivity were investigated. The study showed that a relatively lower temperature, higher pressure and a higher value of H₂:CO₂ mole ratio are favorable for methanol production from CO₂ via the hydrogenation route. The CO₂ conversion improved from 13% to 48% as the pressure increased from 1 bar to 50 bar at an H₂/CO₂ mole ratio of 3. At 50 bar pressure, the CO₂ conversion improved from 48% to 77% with the increase of H₂/CO₂ mole ratio from 3 to 10. However, methanol synthesis at a higher (>5) mole ratio of H₂/CO₂ may not be economi-

cally viable. It was observed that, at 250 °C and 50 bar pressure, the overall process yields around 73% CO₂ conversion, 99.9% CH₃OH selectivity and a negligible (about 1,000 ppm) amount of CO in the outflow with 90% recycling. Furthermore, a techno-economic feasibility study of the methanol synthesis process was performed using an Aspen Plus simulator. The analysis showed that the recycling ratio, feed and product price and plant capacity can play a crucial role in overall plant economics and its sustainability. The study concluded that the proposed process can be economically viable if the H₂ cost is lower than 1,500 \$/ton and/or for a higher (>250 tons/day) throughput capacity.

ACKNOWLEDGEMENTS

The authors express their gratitude to BITS Pilani Hyderabad Campus for providing the necessary support and facilities for the present study.

AUTHOR CONTRIBUTIONS

Suresh Kanuri: Conceptualization, Investigation, Data generation, Writing-original draft; **Jha Deeptank Vinodkumar:** Data generation; **Sounak Roy:** Administration, Data validation; **Chanchal Chakraborty:** Administration, Data validation; **Santanu Prasad Dutta:** Data validation; **Satyapaul A. Singh:** Conceptualization, Result validation, Supervision. Methodology; **Srikanta Dinda:** Conceptualization, Supervision, Writing and editing. All authors read and approved the final manuscript.

CONFLICT OF INTEREST

The authors declare that they have no known competing financial interests or personal relationships that could have appeared to influence the work reported in this manuscript.

NOMENCLATURE

ASPEN PEA : Aspen process economic analyzer

DPBP : discounted payback period

d : discount rate

CEPCI : chemical engineering plant cost index

CF : cash flow

C_{new} : capacity of new equipment

C_{ref} : capacity of reference equipment

DC : direct cost

DCFA : discounted cash flow analysis

FCI : fixed capital investment

IC : indirect cost

IRR : internal rate of return

NPV : net present value

PBP : payback period

P_R : reaction pressure

P_{new} : purchased cost of new equipment

P_{ref} : purchased cost of reference equipment

R : recycling ratio

REquil : equilibrium reactor model

RF : ratio factor

RWGS : reverse-water-gas-shift

S_{MeOH} : methanol selectivity

TCI : total capital investment

TPC : total product cost

TPP : total plant profit

T_R : reaction temperature

WCI : working capital investment

WGS : water-gas-shift

X_{CO_2} : CO₂ conversion

ΔG : Gibbs free energy change

ΔH : enthalpy change

ΔS : entropy change

REFERENCES

1. NESRL ESRL, Available at: https://gml.noaa.gov/ccgg/trends/gl_trend.html.
2. P. S. Murthy, W. Liang, Y. Jiang and J. Huang, *Energy Fuels*, **35**, 8558 (2021).
3. Z. Han, C. Tang, J. Wang, L. Li and C. Li, *J. Catal.*, **394**, 236 (2021).
4. J. Zhang, Z. Li, Z. Zhang, R. Liu, B. Chu and B. Yan, *ACS Sustain. Chem. Eng.*, **8**, 18062 (2020).
5. P. Murge, S. Dinda and S. Roy, *Energy Fuels*, **32**, 10786 (2018).
6. F. Sha, Z. Han, S. Tang, J. Wang and C. Li, *ChemSusChem*, **13**, 6160 (2020).
7. G. Leonzio, E. Zondervan and P. U. Foscolo, *Int. J. Hydrogen Energy*, **44**, 7915 (2019).
8. J. Qaderi, *Int. J. Innov. Res. Sci. Stud.*, **3**, 33 (2020).
9. M.-S. Salehi, M. Askarishahi, F. Gallucci and H. R. Godini, *Chem. Eng. Process. - Process Intensif.*, **160**, 108264 (2021).
10. Z. Cai, J. Dai, W. Li, K. B. Tan, Z. Huang, G. Zhan, J. Huang and Q. Li, *ACS Catal.*, **10**, 13275 (2020).
11. J. Zhong, X. Yang, Z. Wu, B. Liang, Y. Huang and T. Zhang, *Chem. Soc. Rev.*, **49**, 1385 (2020).
12. T. Witton, T. Permsirivanich, W. Donphai, A. Jaree and M. Chareonpanich, *Fuel Process Technol.*, **116**, 72 (2013).
13. A. S. Malik, S. F. Zaman, A. A. Al-Zahrani, M. A. Daous, H. Driss and L. A. Petrov, *Appl. Catal. A Gen.*, **560**, 42 (2018).
14. N. Rui, F. Zhang, K. Sun, Z. Liu, W. Xu, E. Stavitski, S. D. Senanayake, J. A. Rodriguez and C. J. Liu, *ACS Catal.*, **10**, 11307 (2020).
15. S. Kanuri, S. Roy, C. Chakraborty, S. P. Datta, S. A. Singh and S. Dinda, *Int. J. Energy Res.*, **46**, 5503 (2022).
16. R. Gaikwad, A. Bansode and A. Urakawa, *J. Catal.*, **343**, 127 (2016).
17. T. Zou, T. P. Araújo, F. Krumeich, C. Mondelli and J. Pérez-Ramírez, *ACS Sustain. Chem. Eng.*, **10**, 81 (2022).
18. G. Leonzio, *Processes*, **5**, 62 (2017).
19. C. Zhang, K. W. Jun, R. Gao, G. Kwak and H. G. Park, *Fuel*, **190**, 303 (2017).
20. P. Roshia, S. Kumar and H. Ibrahim, *Sustain. Energy Fuels*, **5**, 4336 (2021).
21. F. N. Al-Rowaili, S. S. Khalafalla, D. S. Al-Yami, A. Jamal, U. Ahmed, U. Zahid and E. M. Al-Mutairi, *Chem. Eng. Res. Des.*, **177**, 365 (2022).
22. P. Borisut and A. Nuchitprasittichai, *Front. Energy Res.*, **7**, 1 (2019).
23. K. Atsonios, K. D. Panopoulos and E. Kakaras, *Int. J. Hydrogen*

- Energy*, **41**, 2202 (2016).
24. D. Bellotti, M. Rivarolo, L. Magistri and A. F. Massardo, *J. CO₂ Util.*, **21**, 132 (2017).
25. J. Nyári, M. Magdeldin, M. Larmi, M. Järvinen and A. Santasalo-Aarnio, *J. CO₂ Util.*, **39**, 101166 (2020).
26. M. Son, M. J. Park, G. Kwak, H. G. Park and K. W. Jun, *Korean J. Chem. Eng.*, **35**, 355 (2018).
27. J. H. Jeong, S. Kim, M. J. Park and W. B. Lee, *Korean J. Chem. Eng.*, **39**, 1709 (2022).
28. J. H. Jeong, Y. Kim, S. Y. Oh, M. J. Park and W. B. Lee, *Korean J. Chem. Eng.*, **39**, 1989 (2022).
29. M. Rafati, L. Wang, D. C. Dayton, K. Schimmel, V. Kabadi and A. Shahbazi, *Energy Convers. Manag.*, **133**, 153 (2017).
30. R. Gao, C. Zhang, G. Kwak, Y. J. Lee, S. C. Kang and G. Guan, *Energy Convers. Manag.*, **213**, 112819 (2020).
31. A. I. Osman, N. Mehta, A. M. Elgarahy, M. Hefny, A. A. Hinai, A. H. A. Muhtaseb and D. W. Rooney, *Environ. Chem. Lett.*, **20**, 153 (2022).
32. Y. G. Noh, Y. J. Lee, J. Kim, Y. K. Kim, J. S. Ha, S. S. Kalanur and H. Seo, *Chem. Eng. J.*, **428**, 131095 (2021).
33. N. Pirrone, F. Bella and S. Hernandez, *Green Chem.*, **24**, 5379 (2022).
34. B. Brigljević, M. Byun and H. Lim, *Appl. Energy*, **274**, 115314 (2020).
35. C. V. Miguel, M. A. Soria, A. Mendes and L. M. Madeira, *J. Nat. Gas Sci. Eng.*, **22**, 1 (2015).
36. K. Ahmad and S. Upadhyayula, *Environ. Prog. Sustain. Energy*, **38**, 98 (2019).
37. K. Stangeland, H. Li and Z. Yu, *Ind. Eng. Chem. Res.*, **57**, 4081 (2018).
38. I. U. Din, M. S. Shaharun, M. A. Alotaibi, A. I. Alharthi and A. Naeem, *J. CO₂ Util.*, **34**, 20 (2019).
39. J. Zhong, X. Yang, Z. Wu, B. Liang, Y. Huang and T. Zhang, *Chem. Soc. Rev.*, **49**, 1385 (2020).
40. X. L. Liang, X. Dong, G. D. Lin and H. Bin Zhang, *Appl. Catal. B Environ.*, **88**, 315 (2009).
41. Y. Liu, Y. Zhang, T. Wang and N. Tsubaki, *Chem. Lett.*, **36**, 1182 (2007).
42. X. Chang, X. Han, Y. Pan, Z. Hao, J. Chen, M. Li, J. Lv and X. Ma, *Ind. Eng. Chem. Res.*, **61**, 6872 (2022).
43. Z. Ding, Y. Xu, Q. Yang and R. Hou, *Int. J. Hydrogen Energy*, **47**, 2475 (2022).
44. Z. Lu, K. Sun, J. Wang and Z. Zhang, *Catalysts*, **10**, 1360 (2020).
45. B. Lee, H. S. Cho, H. Kim, D. Lim, W. Cho, C. H. Kim and H. Lim, *J. Environ. Chem. Eng.*, **9**, 106349 (2021).
46. Max S. Peters, Klaus D. Timmerhaus, 5th ed. McGraw-Hill Education (2002).
47. IEA, <https://www.iea.org/data-and-statistics/charts/global-average-levelised-cost-of-hydrogen-production-by-energy-source-and-technology-2019-and-2050>.
48. S. Sadeghi, S. Ghandehariun and M. A. Rosen, *Energy*, **208**, 118347 (2020).